Inter and intra-metamolecular interaction enabled broadband high-efficiency polarization control in metasurfaces

Cong, Longqing; Srivastava, Yogesh Kumar; Singh, Ranjan

2016

Cong, L., Srivastava, Y. K., & Singh, R. (2016). Inter and intra-metamolecular interaction enabled broadband high-efficiency polarization control in metasurfaces. Applied Physics Letters, 108(1), 011110-.

https://hdl.handle.net/10356/82429

https://doi.org/10.1063/1.4939564

Inter and intra-metamolecular interaction enabled broadband high-efficiency polarization control in metasurfaces

Longqing Cong, Yogesh Kumar Srivastava, and Ranjan Singh

Citation: Applied Physics Letters **108**, 011110 (2016); doi: 10.1063/1.4939564
View online: http://dx.doi.org/10.1063/1.4939564
View Table of Contents: http://scitation.aip.org/content/aip/journal/apl/108/1?ver=pdfcov
Published by the AIP Publishing

Inter and intra-metamolecular interaction enabled broadband high-efficiency polarization control in metasurfaces

Longqing Cong,[1,2] Yogesh Kumar Srivastava,[1,2] and Ranjan Singh[1,2,a)]
[1]*Division of Physics and Applied Physics, School of Physical and Mathematical Sciences, Nanyang Technological University, Singapore, Singapore 637371*
[2]*Centre for Disruptive Photonic Technologies, School of Physical and Mathematical Sciences, Nanyang Technological University, Singapore, Singapore 637371*

(Received 12 October 2015; accepted 23 December 2015; published online 7 January 2016)

The near field meta-molecular interactions in a lattice play an important role in determining the collective behavior of the metamaterials. Here, we exploit the nearest neighbor *inter* unit cell interactions and the *intra* near-field coupling in metamolecules to manipulate the co- and the cross-polarized light. We observed large enhancement in the bandwidth and the amplitude of the transmitted light in the strongly coupled meta-molecular lattice. We further show that the proposed metasurface could function as a broadband achromatic quarter-wave plate. The chosen meta-molecular design also enhances the cross-polarized light when integrated with a ground plane to operate in the reflection mode. © *2016 AIP Publishing LLC*. [http://dx.doi.org/10.1063/1.4939564]

The flourishing field of metamaterials has provided a platform to arbitrarily tailor the electromagnetic properties of artificial media and obtain exotic functionalities such as cloaking[1] and negative refraction.[2] Metasurfaces[3,4] are user-defined thin films which rely on periodically or amorphously arranged unit cells with critical dimensions smaller than the operational wavelength. A canonical unit cell design to build the metasurface is a split-ring resonator (SRR) that is usually dubbed as a meta-atom.[5–7] However, different functionalities and spectral properties with larger sophistication fall within reach while constructing the unit cell that consists of coupled meta-atoms to form a metamolecule. There have been several works where the near-field coupling (*intra* coupling) between the meta-atoms in the metamolecules was studied that sustain bright and dark mode coupled resonances.[8,9] The bright mode is directly excited by the external field, while the dark mode is uncoupled from the external field. In addition, the nearest neighbor meta-molecular interaction (*inter* coupling) in a lattice that relies on the periodicity of the array is also important in determining the collective spectral response of the metamaterial devices.[10,11] The period of a meta-atom array has a strong influence on its resonance features, since it determines the nearest neighbor coupling between the individual meta-atoms embedded in a lattice.[12] Here, we exploit this particular feature of a metamaterial array to broaden the bandwidth and enhance transmission efficiencies of the co- and the cross-polarized light through orthogonally twisted meta-atom pair (bright and dark near field coupled) that forms a meta-molecular array in a lattice.

Although the low-loss high quality factor metasurfaces are desirable for many applications, such as lasing spasers,[13] slow light devices,[14] and ultrasensitive sensors,[15] there exist many functionalities that require broadband operation such as polarizers,[16,17] broadband filters,[18,19] wave plates,[20,21] wave deflectors,[22] and perfect electromagnetic absorbers.[23] Several approaches have been followed to enhance the bandwidth of metamaterials including stacking several layers of metasurfaces in the direction of wave propagation.[19,23] Most of the approaches require complex fabrication processes and very precise alignment which limit the large scale manufacturing and the application of such devices. A planar metasurface design that exploits the resonance features of a single surface to achieve a specific functionality does not require complex fabrication steps. However, the resonance of a planar metasurface usually has a narrow resonant bandwidth that can be broadened by enhancing the radiative losses in the metamaterial array. A typical strategy is to couple meta-atoms where the individual resonances of each meta-atom constructively interfere leading to spectral broadening via split resonance modes.[9] In this contribution, we show the broadband operation of a planar metasurface in which the unit cell comprises of *intra* coupled orthogonally twisted meta-atom pair that forms a metamolecule. The chosen metasurface design possesses two coherent radiative loss channels that correspond to both bright and dark meta-atoms.

As shown in Figs. 1(a) and 1(b), we exhibit the zoomed images of the arrays that consists of two orthogonal SRRs in each unit cell fabricated on a double-side polished high resistivity silicon substrate. The samples were fabricated using conventional photolithography, development, metallization, and lift-off processes with aluminum. In our experiments, we kept the distance between the two meta-atoms within the unit cell fixed which actually determines the *intra* coupling in the meta-atom pair. The other geometrical parameters of the SRRs were also kept constant in order to focus on investigating the effect of varying the nearest neighbor *inter* coupling between the metamolecules (a metamolecule here comprises of two meta-atoms in a unit cell) by changing the periodicity in only one direction (y-axis). Here, the lattice period is defined as p_y along the y-axis which is varied from 45 μm to 150 μm and that along x-direction is the period p_x which is kept constant at 150 μm. The fundamental inductive-capacitive (LC) resonance mode can be excited as a bright mode only in one of the meta-atoms with the linearly

a)Email: ranjans@ntu.edu.sg

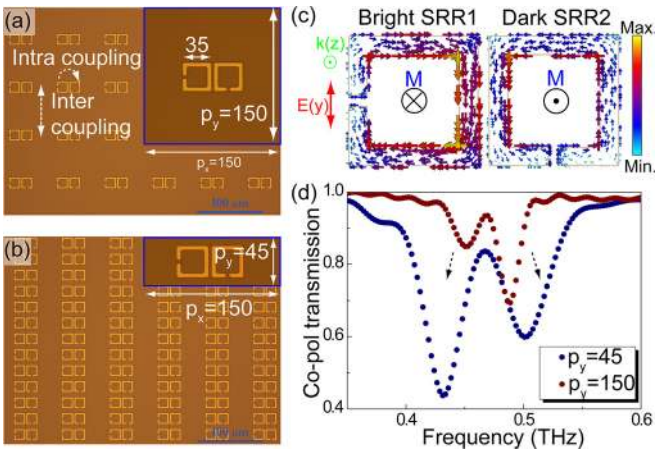

FIG. 1. Images of *intra* coupled meta-molecule and modal interference spectrum. (a) The zoomed image of the fabricated meta-molecule arrays with square lattice $p_x = 150\,\mu$m and $p_y = 150\,\mu$m and (b) the image of the identical exposure area with rectangular lattice constant $p_x = 150\,\mu$m and $p_y = 45\,\mu$m. (c) The surface current distribution with TE excitation at the fundamental resonance mode and the corresponding bright and dark meta-atoms. (d) The co-polarized transmission spectra corresponding to the planar array with square and rectangular lattice.

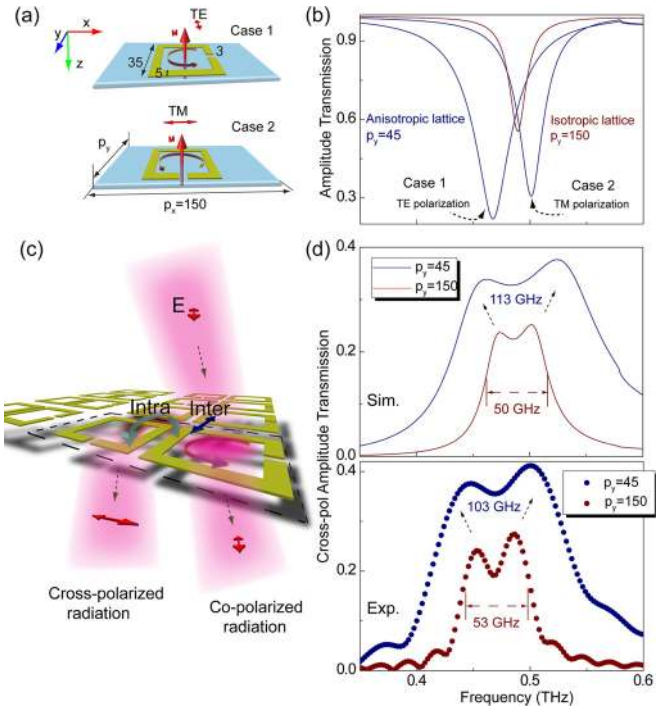

FIG. 2. Fundamental modes of single SRR and cross-polarized transmission spectra of a meta-molecule array. (a) Individual SRR1 and SRR2 are placed on a rectangular substrate. (b) The simulated transmission spectra of the single SRR array for two cases. (c) The schematic diagram of the meta-molecule array with linearly polarized illumination. (d) The simulated and measured cross-polarized transmission of the meta-molecule with varied $p_y = 45$ to $150\,\mu$m and fixed $p_x = 150\,\mu$m.

polarized incidence. The resonant bright meta-atom acts as a magnetic dipole as a result of bianisotropy of SRR. The *intra* near-field coupling from the bright SRR to the dark SRR occurs only through the magnetic dipole where the electric coupling is forbidden due to the orthogonally twisted SRR configuration in the meta-molecular system. In order to visualize the bianisotropy of SRR,[24,25] CST Microwave Studio was employed to simulate the surface current distributions as shown in Fig. 1(c). It is clearly observed that a current loop is directly induced in SRR1 by the pure electric excitation with linearly polarized incidence along *y*-axis (E_y) and wave vector along *z*-axis (TE mode). Such a current loop would then contribute to form the out-of-plane magnetic dipole which inductively excites the fundamental resonance in dark SRR2. The radiation of dark meta-atom will interfere with the bright resonance in the co-polarized transmission spectra as shown in Fig. 1(d). Meanwhile, due to the orthogonal orientation of the dark meta-atom (SRR2) relative to the bright one (SRR1), the polarization of the radiation emanating from the dark atom would be orthogonal to the bright one, i.e., the cross-polarized radiation (radiation polarized along *x*-axis with *y*-polarized incidence, t_{xy}). The cross-polarized spectrum also exhibits the mode interference which is similar in nature to the co-polarized transmission. The effect of *intra* coupling in the co-polarized regime has been thoroughly investigated in the previous works where the resonance features mainly rely on the spatial distance between meta-atoms which determines the coupling strength between them. However, the influence of *inter* coupling and anisotropy that mainly depend on the periodicity of the meta-molecular array have not been investigated so far. Therefore, we designed a series of metamolecules with varied periodicity as shown in Figs. 1(a) and 1(b) to thoroughly study the effects of *inter* coupling in the meta-molecular system and its impact on controlling the polarization state.

In order to clearly interpret the impact of *inter* coupling in the meta-molecular system, we first show the fundamental resonance mode of the individual meta-atom with the same lattice constant that excludes the effects of *intra* coupling. The two scenarios are schematically explained in Fig. 2(a). As shown in Fig. 2(b), both the cases exhibit identical isotropic resonance response for square lattice with periodicity $p_x = p_y = 150\,\mu$m. However, their responses differ when the lattice becomes rectangular (see Fig. 2(b)) by reducing the *y* direction period to $p_y = 45\,\mu$m while p_x is kept constant at $150\,\mu$m. Comparing the two cases of orthogonal direction excitation (TE and TM) for a fixed rectangular lattice where the same number of unit cells are excited in an identical illumination area, the rectangular lattice induced anisotropy plays a key role in determining the resonance response of individual SRR in a unit cell. The anisotropy results in the shift of eigen LC resonance frequencies with orthogonally polarized excitations. While comparing the resonances with different lattice periods, i.e., $p_y = 45\,\mu$m and $p_y = 150\,\mu$m, the eigen resonance frequency also shifts which actually originates from the nearest neighbour *inter* unit cell coupling. In addition, the resonance amplitude becomes stronger for $p_y = 45\,\mu$m due to the higher unit cell packing density.[12] Therefore, the two prominent effects of *inter* unit cell nearest neighbor coupling occur on the eigen LC resonance of the individual SRR array: (a) shift of LC resonance frequency due to anisotropic rectangular lattice and (b) the modulation of the resonance amplitude due to the varied packing density.

Once the identical meta-atoms are arranged orthogonally within a unit cell to form a metamolecule, as schematically shown in Fig. 2(c), the spectral mode interference

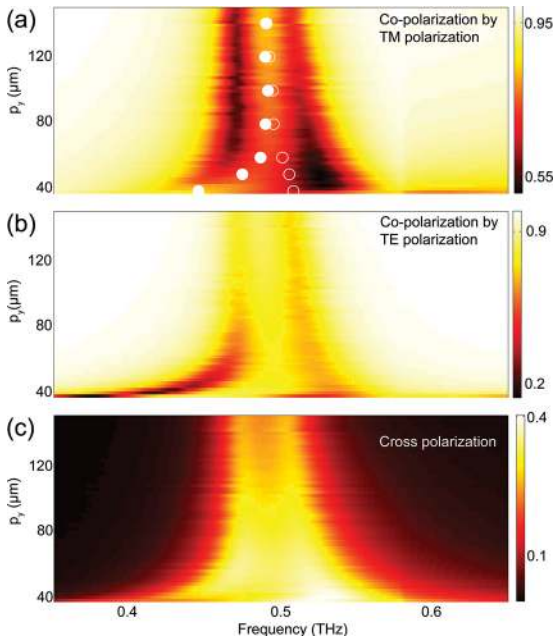

FIG. 3. The amplitude transmission of the meta-molecule with varying lattice constant. The co-polarized amplitude transmission of meta-molecule array with (a) TM polarization and (b) TE polarization excitation. (c) The cross-polarized transmission of the meta-molecule array. The inset points are the eigen frequencies of the individual meta-atom array in the corresponding lattice constant.

occurs. With the linearly polarized incidence, both the radiative channels from bright and dark meta-atoms are excited. As revealed by the co-polarized transmission in Fig. 1(d), the transmission bandwidth of the meta-molecular array is broadened due to the fundamental mode splitting caused by the near field *intra* coupling between the meta-atoms within each unit cell. Similar to the co-polarized transmission, the cross-polarized spectra also reveal the mode interference and broadened resonance in Fig. 2(d). In line with the reciprocity theorem, the absence of an external magnetic field would ensure that the two cross-polarized components (t_{xy}, t_{yx}) in the Jones matrix show identical behaviors; therefore, we simply consider one of the components. The top and bottom windows in Fig. 2(d) exhibit the simulated and measured data for the cross-polarized transmission that reveal good agreement.

In experiments, we employed the 8–*f* antenna based terahertz time-domain spectroscopy (THz-TDS) system[26] with a set of polarizers inserted to coherently measure the co- and cross-polarized transmission signals. We obtained the time-domain electric field waveforms and then performed Fourier transform to obtain the frequency domain spectra with both amplitude and phase information. The transmission amplitude spectra $|\tilde{t}_{ji}(\omega)|$ and phase information $\phi_{ji}(\omega)$ are obtained by $\tilde{t}_{ji}(\omega) = \tilde{t}_{ji}^{Sam}(\omega)/\tilde{t}_{ji}^{Ref}(\omega)$, where $\tilde{t}_{ji}^{Sam}(\omega)$ is the complex transmitted signal of sample and $\tilde{t}_{ii}^{Ref}(\omega)$ is the complex transmitted reference signal, respectively. Here, the reference is the same blank silicon as the substrate and i and j represent the input (incident) and output polarization states. All the measurements were performed at normal incidence in dry nitrogen atmosphere. The cross-polarized transmission component has recently been shown to have promising applications in arbitrarily manipulating the wave front[27] and realizing the flat lens in the transmission mode.[3] The bandwidth as well as the conversion efficiency of the cross-polarized light are extremely important for designing highly efficient devices. Therefore, it is important to improve the performance of cross-polarized component which was accomplished in our current experiments. As shown in Fig. 2(d), there is strong amplitude enhancement at the fundamental split modes for the cross-polarized transmission signal. The 3 dB bandwidth of cross-polarized transmission is 53 GHz, when the lattice is a square with $p_y = p_x = 150\ \mu$m. As the lattice constant p_y is changed to 45 μm ($p_x = 150\ \mu$m), the effects of a rectangular anisotropic lattice on the eigen frequencies of the two bright and dark SRRs appear for the coupled meta-molecular array. The anisotropy causes the fundamental resonance modes of individual SRRs to move spectrally apart which plays a dominant role in broadening the resonant bandwidth of the cross-polarized light as revealed in Fig. 2(d) where the 3 dB bandwidth is nearly doubled to 103 GHz. In addition to the bandwidth broadening effect, the resonance amplitude is also modulated by adjusting the lattice period that changes the number of illuminated metamolecules. We could visibly observe the different densities of metamolecules from the images in Figs. 1(a) and 1(b). As p_y is decreased to 45 μm, the cross-polarized transmission amplitude is enhanced from 0.26 to 0.42 in the resonance band of interest. Similar effects are also observed in the co-polarized transmission spectra as shown in Fig. 1(d). The broadened resonance enhances the operation bandwidth, and the increase in the amplitude leads to a higher conversion efficiency for potential applications in polarization based metadevices.

In order to visualize the spectral evolution with the change in p_y upon being varied from 150 μm to 40 μm in steps of 5 μm, we plotted the co- and cross-polarized spectra of the *intra* coupled metamolecules in Fig. 3. The fundamental LC resonance frequencies of the individual meta-atom array SRR1 (dot) and SRR2 (circle) in the corresponding lattice periods are also shown in the graph for reference where the rectangular lattice induced anisotropy is obvious from the split of the frequency as p_y decreases. Consistent with the fundamental eigen resonance frequency split of individual meta-atom array, the bandwidth of the *intra* coupled meta-molecule broadens in both co- and cross-polarized spectra, while the lattice period is decreased from $p_y = 150\ \mu$m to $p_y = 40\ \mu$m. The change in periodicity leads to the change in the *inter* unit cell coupling along the *y*-axis. The broadening of the bandwidth in fact originates from the modal superposition of the orthogonally twisted SRRs. While $p_y = p_x = 150\ \mu$m, the fundamental resonance frequencies of SRR1 and SRR2 arrays have strong overlap, and the interference in the metamolecule causes the mode splitting in the transmission spectrum. However, when the lattice induced anisotropy kicks in for $p_y < p_x$, the spectral separation between the fundamental resonance frequencies of individual SRR1 and SRR2 increases as p_y becomes smaller. This leads to the modal superposition in the meta-molecular system which enhances the operation bandwidth of the *intra* and *inter* unit cell coupled metamolecule. In addition, the enhancement of the amplitude is also clearly visible in Fig. 3.

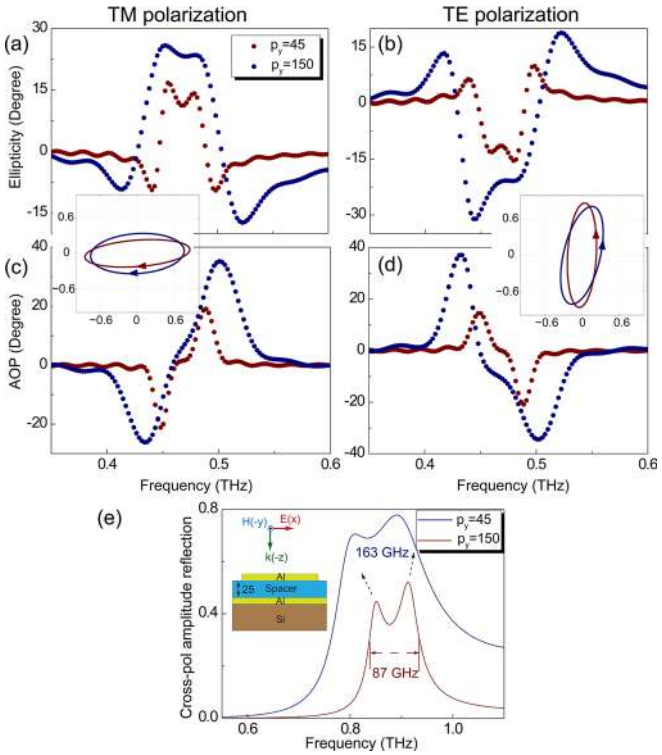

FIG. 4. The calculated polarization parameters. The ellipticity of output light with different periodicity by (a) TM polarization and (b) TE polarization excitations. The angle of polarization ellipse with different periodicity by (c) TM polarization and (d) TE polarization. Insets are the corresponding polarization states at 0.47 THz. (e) Metasurface integrated into a three layer design to enhance the conversion efficiency of the reflected cross-polarized component.

With the cross-polarized component radiated to the far-field, the polarization state of the output light is modulated. To demonstrate the device functionalities, we calculated the ellipticity (χ) and the angle of polarization ellipse (AOP, α) of the output light according to Stokes parameters.[28,29] The ellipticity $\chi = 45^\circ$ indicates a perfect right-handed circularly polarized (RCP) light; $\chi = -45^\circ$ indicates a perfect left-handed circularly polarized (LCP) light; and $-45^\circ < \chi < 45^\circ$ represents elliptically (linearly, $\chi = 0^\circ$) polarized light. AOP describes the rotation of the main axis of the polarization ellipse that is a measure of the circular birefringence. As shown in Fig. 4, we clearly observe the bandwidth enhancement of ellipticity spectra when the periodicity is adjusted from $p_y = 150$ to $p_y = 45\,\mu$m and AOP is non-zero due to the emergence of the cross-polarized component. In addition, the degrees of ellipticity and AOP are both enhanced for the decreased periodicity in which a larger number of metamolecules are excited. The highest AOP approaches 35° with the ellipticity of about 0° at 0.43 THz for *y*-polarized incidence which indicates a perfect linear polarization rotation by the metasurface. The ellipticity approaches −30° at 0.46 THz with *y*-polarized incidence whose resultant polarization states are shown as insets of Fig. 4. The broadband large-value ellipticity highlights the potential of a simple metasurface device to function as an achromatic quarter wave plate. Although the AOP is enhanced to approach 35° at a specific frequency, the broadband operation is not allowed in the metasurface configuration which mainly relies on the amplitude of the cross-polarized component. We provide another scheme to enhance the amplitude of the cross-polarized light as discussed below.

By integrating the metasurface into a reflection configuration by adding a dielectric spacer and a ground plane as shown in the inset of Fig. 4(e), the high-efficiency broadband conversion of cross-polarized component becomes possible.[30] Usually, only the co-polarized radiative channel is preferred, which dissipates the energy through the radiative and the ohmic losses to realize the perfect absorbance. However, the cross-polarized radiative channel would be strongly enhanced while combining the orthogonally oriented meta-atoms into the meta-molecular array.[31] As shown in Fig. 4(e), the reflected cross-polarized amplitude is enhanced to a value of 0.45 with the 3 dB bandwidth of 87 GHz for the metamolecule with $p_y = 150\,\mu$m and the spacer thickness of $25\,\mu$m. Similarly, both the operation bandwidth and amplitude could be enhanced as the periodicity is adjusted to $p_y = 45\,\mu$m, where the amplitude is enhanced to larger than 0.7 with 3 dB bandwidth being almost doubled to about 163 GHz. Such a three layered device design that operates in the reflection mode has potential to function as a broadband, high-efficiency half-wave plate by appropriately tailoring the *intra* meta-atom and *inter* meta-molecular coupling along with the optimized spacer thickness to suppress the co-polarized reflection, and thus broadband, high-value AOP would be achievable.

In summary, we have studied the *inter* unit cell coupling effect in a meta-molecular array that consists of *intra* near-field coupled bright and dark meta-atoms. We exploit both coupling mechanisms to enhance the resonance bandwidth and the intensity of the co- and cross-polarized terahertz light. The modal superposition of the coherent radiative modes enables broadband operation in the orthogonally twisted meta-molecular array. By engineering the periodicity, the lattice anisotropy is tailored to broaden the transmission bandwidth. Additionally, the resonant amplitude is also proportional to the periodicity that determines the illuminated number of unit cells in a large meta-molecular array. The proposed meta-molecular design has the potential to operate as an achromatic wave plate; and the cross-polarization conversion efficiency can be further improved by integrating the metasurface with a dielectric spacer and a ground plane so that the device operates in a reflection configuration. Such a manipulation of the polarization state of the terahertz waves would enable future terahertz polarization sensitive devices and technologies.

The authors acknowledge NTU startup Grant No. M4081282, MOE Tier 1 Grant No. M4011362, and MOE Grant No. MOE2011-T3-1-005 for funding of this research.

[1]D. Schurig, J. Mock, B. Justice, S. A. Cummer, J. B. Pendry, A. Starr, and D. Smith, Science **314**, 977 (2006).
[2]J. B. Pendry, Phys. Rev. Lett. **85**, 3966 (2000).
[3]L. Cong, M. Manjappa, N. Xu, I. Al-Naib, W. Zhang, and R. Singh, Adv. Opt. Mater. **3**, 1537 (2015).
[4]R. Singh, X. Lu, J. Gu, Z. Tian, and W. Zhang, J. Opt. **12**, 015101 (2010).
[5]T.-J. Yen, W. Padilla, N. Fang, D. Vier, D. Smith, J. Pendry, D. Basov, and X. Zhang, Science **303**, 1494 (2004).
[6]W. J. Padilla, A. J. Taylor, C. Highstrete, M. Lee, and R. D. Averitt, Phys. Rev. Lett. **96**, 107401 (2006).
[7]R. A. Shelby, D. R. Smith, and S. Schultz, Science **292**, 77 (2001).

[8]W. Cao, R. Singh, C. Zhang, J. Han, M. Tonouchi, and W. Zhang, Appl. Phys. Lett. **103**, 101106 (2013).
[9]R. Singh, I. Al-Naib, D. R. Chowdhury, L. Cong, C. Rockstuhl, and W. Zhang, Appl. Phys. Lett. **105**, 081108 (2014).
[10]N. Xu, R. Singh, and W. Zhang, J. Appl. Phys. **118**, 163102 (2015).
[11]R. Singh, C. Rockstuhl, and W. Zhang, Appl. Phys. Lett. **97**, 241108 (2010).
[12]V. Fedotov, N. Papasimakis, E. Plum, A. Bitzer, M. Walther, P. Kuo, D. Tsai, and N. Zheludev, Phys. Rev. Lett. **104**, 223901 (2010).
[13]N. I. Zheludev, S. Prosvirnin, N. Papasimakis, and V. Fedotov, Nat. Photonics **2**, 351 (2008).
[14]M. Manjappa, S.-Y. Chiam, L. Cong, A. A. Bettiol, W. Zhang, and R. Singh, Appl. Phys. Lett. **106**, 181101 (2015).
[15]L. Cong, S. Tan, R. Yahiaoui, F. Yan, W. Zhang, and R. Singh, Appl. Phys. Lett. **106**, 031107 (2015).
[16]L. Cong, W. Cao, X. Zhang, Z. Tian, J. Gu, R. Singh, J. Han, and W. Zhang, Appl. Phys. Lett. **103**, 171107 (2013).
[17]Y. Zhao, M. Belkin, and A. Alù, Nat. Commun. **3**, 870 (2012).
[18]N. Han, Z. Chen, C. Lim, B. Ng, and M. Hong, Opt. Express **19**, 6990 (2011).
[19]X. Zhang, J. Gu, W. Cao, J. Han, A. Lakhtakia, and W. Zhang, Opt. Lett. **37**, 906 (2012).
[20]L. Cong, N. Xu, J. Gu, R. Singh, J. Han, and W. Zhang, Laser Photonics Rev. **8**, 626 (2014).
[21]L. Cong, N. Xu, J. Han, W. Zhang, and R. Singh, Adv. Mater. **27**, 6630 (2015).
[22]X. Zhang, Z. Tian, W. Yue, J. Gu, S. Zhang, J. Han, and W. Zhang, Adv. Mater. **25**, 4567 (2013).
[23]F. Ding, Y. Cui, X. Ge, Y. Jin, and S. He, Appl. Phys. Lett. **100**, 103506 (2012).
[24]R. Marqués, F. Medina, and R. Rafii-El-Idrissi, Phys. Rev. B **65**, 144440 (2002).
[25]H. Tao, A. Strikwerda, K. Fan, W. Padilla, X. Zhang, and R. Averitt, Phys. Rev. Lett. **103**, 147401 (2009).
[26]D. Grischkowsky, S. Keiding, M. van Exter, and C. Fattinger, J. Opt. Soc. Am. B **7**, 2006 (1990).
[27]N. Yu, P. Genevet, M. A. Kats, F. Aieta, J.-P. Tetienne, F. Capasso, and Z. Gaburro, Science **334**, 333 (2011).
[28]D. Goldstein and D. H. Goldstein, *Polarized Light, revised and expanded* (CRC Press, 2011).
[29]L. Cong, N. Xu, W. Zhang, and R. Singh, Adv. Opt. Mater. **3**, 1176 (2015).
[30]N. Landy, S. Sajuyigbe, J. Mock, D. Smith, and W. Padilla, Phys. Rev. Lett. **100**, 207402 (2008).
[31]Y. Yang, W. Wang, P. Moitra, I. I. Kravchenko, D. P. Briggs, and J. Valentine, Nano Lett. **14**, 1394 (2014).